



## Determination of the radial profile of the photoelastic coefficient of plastic optical fibers

S. Acheroy<sup>1\*</sup>, T. Geernaert<sup>2</sup>, H. Ottevaere<sup>2</sup>, H. Thienpont<sup>2</sup>, D.J. Webb<sup>3</sup>, C.A.F Marques<sup>4</sup>, P. Gang-ding<sup>5</sup>, M. Pawel<sup>6</sup>, F. Berghmans<sup>2</sup>

- 1 Royal Military Academy, Dept of Communication, Information, Systems and Sensors (CISS), Ave Renaissance 30, 1000 Brussels, Belgium
- 2 Vrije Universiteit Brussel, Dept. of Applied Physics and Photonics, Brussels Photonics Team (B-PHOT), Pleinlaan 2, B-1050 Brussels, Belgium
- 3 Aston Institute of Photonic Technologies, Aston University, Aston Triangle, B4 7ET Birmingham, UK
- 4 Instituto de Telecomunicações and University of Aveiro Physics Department & I3N, Campus de Santiago, 3810-193 Aveiro, Portugal
- 5 Photonics & Optical Communications, School of Electrical Engineering & Telecommunications, University of New South Wales, Sydney 2052, NSW, Australia
- 6 Laboratory of Optical Fibers Technology, Maria Curie Skłodowska University Skłodowska Sq 3, 20-031 Lublin, Poland

\*Corresponding author: sophie.acheroy@rma.ac.be

**Abstract:** We developed a measurement method to determine the radial distribution of the photoelastic coefficient  $C(r)$  in step-index polymer optical fibers (POFs). The method is based on the measurement of the retardance profile of a transversally illuminated fiber for increasing tensile load. The radial profile  $C(r)$  is obtained from the inverse Abel transform of this retardance profile. We measured polymer fibers from different manufacturers. The radial profile of the photoelastic constant can considerably vary depending on the type and treatment of POFs, even when made from similar materials, which leads to the conclusion that the photoelastic constant should be characterized for each different type of POF. The impact of annealing the fiber samples on  $C(r)$  is also addressed.

### 1. Introduction

In the field of optical sensors, polymer optical fibers (POFs) provide an interesting alternative for their glass counterparts, owing to their specific characteristics compared to glass fibers. For example, they feature higher elastic limits and can be made from biocompatible materials [1–3]. Simulating and predicting the response of physical or dynamometric optical fiber sensors to externally applied mechanical load requires good knowledge of the fiber material parameters. In this respect it is well known that the photoelastic effect plays a crucial role in glass and polymer fibers, when these are used as transducers for mechanical quantities such as stress, strain and pressure. More particularly, it is important to use correct values of the stress-optic coefficients  $C_1$  and  $C_2$  [ $\text{Pa}^{-1}$ ] and of the photoelastic coefficient  $C = C_1 - C_2$  when calculating the response of optical fibers to mechanical load, since these parameters link the applied stress to the change of the refractive index in the fiber. In this paper we describe a method to determine the photoelastic coefficient in POFs. More specifically, we experimented with fibers drawn from polymethylmethacrylate (PMMA) as that material is most commonly used to manufacture polymer fibers. The value of  $C$  for PMMA reported in the literature varies significantly from  $-1.08 \times 10^{-10} \text{ Pa}^{-1}$  to  $5.3 \times 10^{-12} \text{ Pa}^{-1}$  [4–8]. In the particular case POFs, the drawing conditions and presence of dopants in the polymer could influence the value of the photoelastic constant and lead to the necessity to measure the value of  $C$  for each type of POF. The measurement methods to determine  $C$  in glass and polymer proposed in the literature rely on the hypothesis that  $C$  is constant throughout the fiber section but making such assumption is not straightforward [9, 10]. Therefore we also attempted to determine the radial distribution of the photoelastic constant  $C(r)$  in PMMA fibers before and after a specific annealing process. In section 2 we describe the measurement method. The measurement results on the POFs before and after annealing are presented and discussed in the third section. Section 4 closes our article with a summary of our findings.

### 2. Presentation of the measurement method

#### 2.1 Retardance measurement

The determination of  $C(r)$  requires the measurement of the retardance profile of a transversally illuminated fiber as a function of the tensile load applied to the fiber. The inverse Abel transform of the retardance allows



obtaining  $C(r)$ . In previous publications we have detailed the measurement method to obtain the retardance profile of the fiber [11, 12]. We recall the main steps below for the sake of completeness.

We subject the fiber to a known axial load  $\sigma_z$ . We assume that the load is constant across the fiber section. We measure the retardance for tensile stress values varying from 10 MPa to 50 MPa. To do so the fiber is illuminated with monochromatic light at 633 nm, linearly polarized light at 45°C with respect to the fiber axis. As illustrated in Figure 1 the wave vector of the light is perpendicular to the fiber axis and parallel with the x-axis. The fiber is immersed in index matching liquid to avoid refraction at the boundaries of the optical fiber.

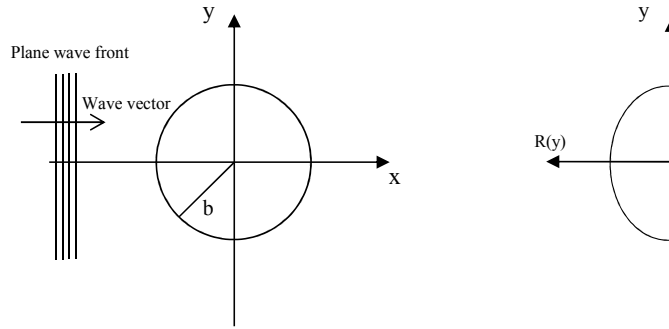


Figure 1: Illustration of an optical fiber transversely illuminated with a plane wave (left) and resulting retardance profile  $R(y)$  (right).  $b$  is the radius of the fiber. The  $z$ -axis is taken along the fiber length with a direction exiting the page.

The axial load applied to the fiber induces birefringence in the fiber material. The two linearly polarized components along the  $y$  and  $z$  directions will experience a different phase shift that can be observed as the projected retardance  $R(y)$  between these two orthogonal components. The projected retardance  $R(y)$  is related to the axial stress by an inverse Abel transform [13–15], as given by equation (1):

$$\sigma_z \times C(r) = -\frac{1}{\pi} \int_r^b \frac{dR(y) / dy}{\sqrt{y^2 - r^2}} dy \quad (1)$$

The photo-elastic constant  $C(r)$  is the regression coefficient linking the inverse Abel transform of the projected retardance  $R(y)$  and the applied known axial stress  $\sigma_z$ .  $r$  is the radial distance taken from the fiber's center and  $b$  is the radius of the fiber. To obtain the radial profile of the photoelastic constant  $C(r)$ , we use a polarizing microscope and apply the Sénarmont compensation method to measure the full-field view of  $R(y)$ .

### 2.1 Inverse Abel transform

In a previous publication [16] we have introduced two algorithms to compute the inverse Abel transform. Both algorithms are based on Fourier theory but the approach is somehow different. In the first algorithm we expand the measured retardance  $R(y)$ , corresponding to a specific value of the axial load, in Fourier series. We compute the inverse Abel transform of the expansion of  $R(y)$  and we obtain equation (2).

$$\sigma_z \times C(r) = -\frac{\pi}{2b} \sum_{k=1}^{k_{\max}} a_k k \frac{2}{\pi} \int_0^{\sqrt{1-\rho^2}} (t^2 + \rho^2)^{-1/2} \times \sin(k\pi\sqrt{t^2 + \rho^2}) dt \quad (2)$$

where  $\rho = r / b$  is the normalized radius,  $t = \sqrt{1 - \rho^2}$  and  $a_k$  is the  $k^{\text{th}}$  Fourier coefficient of the Fourier series of the retardance.

In the second algorithm we expand the result  $C(r) \cdot \sigma_z$  of the inverse Abel transform in Fourier series. The expression of the expansion is given in equation (3).



$$[\sigma_z \times C(r)]_F = a_0 + \sum_{k=1}^{\infty} a_k \cos(k\pi \frac{r}{b}) \quad (3)$$

The forward Abel transform of the expansion yields the measured retardance. The expression of the retardance becomes (4).

$$R_F(y) = b.a_0 \int_0^{\sqrt{1-\rho^2}} dt + b \sum_{k=1}^{\infty} a_k \int_0^{\sqrt{1-\rho^2}} \cos(k\pi \sqrt{t^2 + \rho^2}) dt \quad (4)$$

where  $\rho = x/b$  is the normalized radius and  $t = \frac{\sqrt{r^2 - y^2}}{b}$ . To determine the amplitude of the Fourier

coefficients  $a_k$  in equation (4),  $R_F(y)$  is compared to the measured retardance by applying the least square criterion. The main difference between the two algorithms is the presence of a constant term in the expansion of  $\sigma_z \times C(r)$  in the second algorithm. It allows the algorithm to converge with a lower amount of Fourier coefficients. Moreover, the first algorithm requires the integration of a derivative, which is very sensitive to measurement noise. To establish the radial distribution of the photoelastic constant, we have demonstrated in [16] that both algorithms are fully equivalent, but that the first algorithm requires a larger amount of Fourier coefficients. If we consider increased measurement noise, the influence of the noise on the inverse Abel transform becomes predominant and a large number of Fourier coefficients leads to very noisy shapes. In that case the amount of considered coefficients has to be reduced and  $C(r)$  should then be calculated with the second algorithm.

### 3. Measurement results and discussion

We have measured  $C(r)$  of five singlemode polymer fibers. The description of the composition and specific fabrication process of each fiber has already been detailed in a previous publication [17]. We summarize the main characteristics of the fibers in Table 1.

Table 1: Main characteristics and of the polymer optical fibers used to measure the retardance and determine the radial profile of the photoelastic coefficient [18–20]. The mean measured value of  $C$  on the unannealed and annealed fibers are also mentioned

Fiber	Type	$d_{\text{core}}$	$d_{\text{cladding}}$	Thermal treatment of the preform	Drawing Temperature	C unannealed [ $\times 10^{-12}$ Pa $^{-1}$ ]	C annealed at 80°C [ $\times 10^{-12}$ Pa $^{-1}$ ]
1	PMMA	10 $\mu\text{m}$	110 $\mu\text{m}$	45°C to 75°C within 4 days	220°C	0,047	1,23
2	PMMA	10 $\mu\text{m}$	133 $\mu\text{m}$	45°C to 75°C within 4 days	220°C	-0,93	1,50
3	PMMA	12 $\mu\text{m}$	260 $\mu\text{m}$	36°C to 88°C within 4,5 days	225°C	0,504	1,57
4	PMMA	9 $\mu\text{m}$	110 $\mu\text{m}$	*	*	-0,15	1,54
5	PMMA	4 $\mu\text{m}$	210 $\mu\text{m}$	80°C during 2 weeks	290°C	3,85	3,94

\*The thermal treatment of the preform and the drawing temperature have not been communicated by the manufacturer.

We have determined  $C(r)$  for the pristine samples. We then annealed the samples for 8 hours at 80°C and we have determined the mean value of  $C$  and  $C(r)$  following each annealing step. The influence of annealing the fibers at 80°C for 8 hours is clearly visible. The results are shown in Figure 2 and the mean values of the measured  $C$  are also summarized in Table 1. There is no specific annealing treatment of the preform for Fibers 1, 2 and 3. We can assume that there was no specific temperature treatment for the commercially available Fiber 4. Our findings evidence the impact of annealing at a higher temperature. The variance decreases in all fibers that did not benefit from a specific temperature treatment of the preform, which explains a smoother shape of  $C(r)$ . The annealing process increases significantly the value of  $C(r)$  towards a comparable mean value. Note that the overshoot at  $r = 0$ , i.e. in the center of the fiber, correspond to a numerical artefact of the inverse Abel transform. The height of the overshoot depends on the amount of Fourier coefficients considered in the expansion of the inverse Abel transform, as we explained in details in [12], and cannot be related to an actual property of the optical fiber. The radial profile of  $C(r)$  for fiber 5 is not affected by the annealing process. The preform of that fiber has been annealed for 2 weeks at 80°C prior to drawing. We find a mean value for  $C$  of  $4 \times 10^{-12}$  Pa $^{-1}$ , which is larger than the values we measured for Fibers 1 to 4.

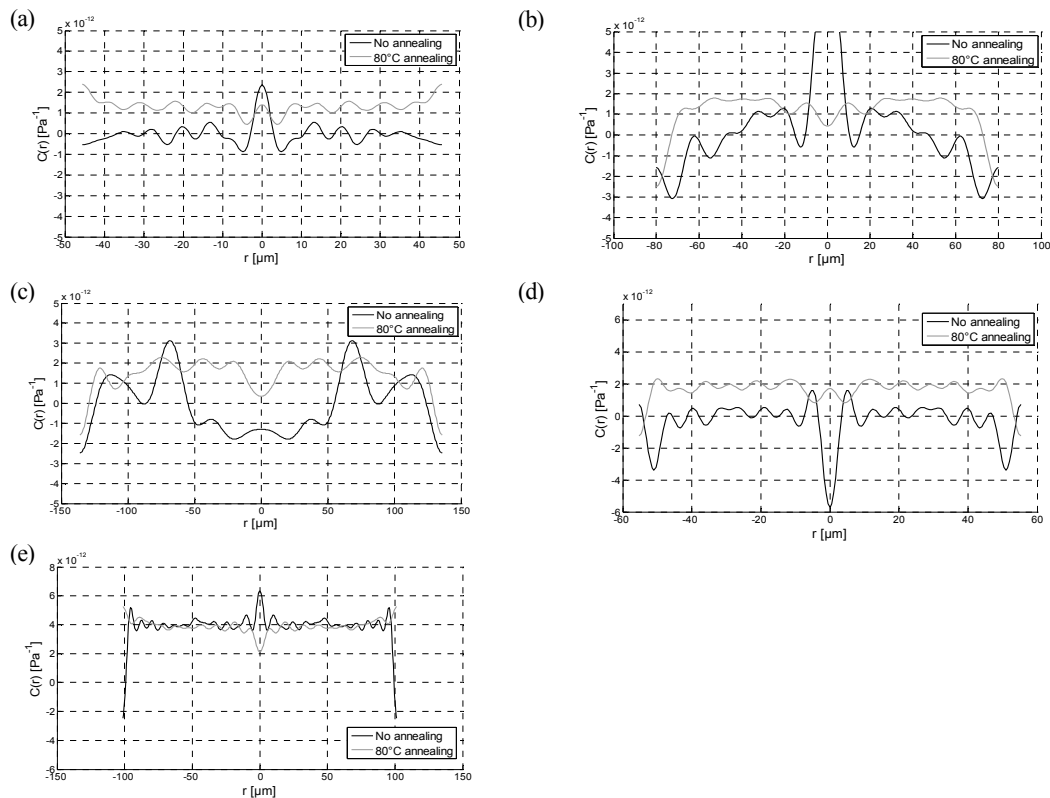


Figure 2 Comparison of the radial distribution of the photoelastic coefficient  $C(r)$  of the POFs under test without annealing and with 8 hours annealing at 80°C in (a) Fiber 1, (b) Fiber 2, (c) Fiber 3, (d) Fiber 4 and (e) Fiber 5 .

#### 4. Conclusion

We have measured the radial distribution of the photoelastic constant  $C(r)$  in five types of PMMA optical fibers. The same distribution has been measured again after an annealing treatment of 8 hours at 80°C.

To do so we determined the retardance of the laterally illuminated fibers. We obtained a full field view of the retardance with the use of a polarizing microscope. We applied two algorithms based on Fourier theory to calculate the inverse Abel transform of the measured retardance. The first algorithm decomposes the measured retardance in Fourier series before to performing the inverse Abel transform, whilst the second algorithm expands the desired radial profile and then computes the forward Abel transform. The result of that operation is then compared to the measured retardance profile. The main conclusion is that the second algorithm is more robust when one has to deal with noisy data.

We found the measured photoelastic constants  $C$  of the five samples of PMMA fibers to be very different. This indicates that  $C$  cannot be approximated by any standard value. Moreover, the annealing treatment of fibers 1 to 4 significantly increases  $C$  and yields a more regular and smooth profile  $C(r)$ . This may indicate a reduced variation of the material parameter  $C$  across the fiber section and an increased homogeneity in the cross-section of the POF. The effect of annealing on Fiber 5, of which the preform has been annealed prior to drawing, is different. This fiber is much less sensitive to thermal treatment and the mean value of  $C$  is much higher.



## 5. Acknowledgements

This work was partially supported by the IWT-SBO Project with Contract 120024 ‘Self Sensing Composites - SSC’. T. Geernaert is post-doctoral research fellow with the Research Foundation Flanders (FWO). The authors would also like to acknowledge financial support from the Methusalem and Hercules Foundations. The Belgian Science Policy Interuniversity Attraction Pole P7/35 is acknowledged as well. Carlos A.F. Marques was supported by Marie Curie Intra European Fellowship included in the 7th Framework Program of the European Union (project PIEF-GA-2013-628604) and FCT Fellowship (SFRH/BPD/109458/2015).

## 6. References

- [1] N. G. Harbach, “Fiber bragg gratings in Polymer Optical Fibers,” EPFL, 2008.
- [2] K. Peeters, “Polymer optical fibre sensors - A review,” *Smart Mater. Struct.*, vol. 20, no. 013002, 2011.
- [3] F. Berghmans and H. Thienpont, “Plastic Optical Fibers for Sensing Applications,” *OFC*, pp. 3–5, 2014.
- [4] W. Xu, X. F. Yao, H. Y. Yeh, and G. C. Jin, “Fracture investigation of PMMA specimen using coherent gradient sensing (CGS) technology,” *Polym. Test.*, vol. 24, pp. 900–908, 2005.
- [5] R. M. Waxler, D. Horowitz, and A. Feldman, “Optical and physical parameters of Plexiglas 55 and Lexan,” *Appl. Opt.*, vol. 18, no. 1, pp. 101–104, 1979.
- [6] A. Tagaya, L. Lou, Y. Ide, Y. Koike, and Y. Okamoto, “Improvement of the physical properties of poly(methyl methacrylate) by copolymerization with N-pentafluorophenyl maleimide; zero-orientational and photoelastic birefringence polymers with high glass transition temperatures,” *Sci. China Chem.*, vol. 55, no. 5, pp. 850–853, 2012.
- [7] A. Tagaya, H. Ohkita, T. Harada, K. Ishibashi, and Y. Koike, “Zero-birefringence optical polymers,” *Macromolecules*, vol. 39, pp. 3019–3023, 2006.
- [8] F. Ay, A. Kocabas, C. Kocabas, A. Aydinli, and S. Agan, “Prism coupling technique investigation of elasto-optical properties of thin polymer films,” *J. Appl. Phys.*, vol. 96, no. 12, pp. 7147–7153, 2004.
- [9] A. Bertholds and B. Dändliker, “Determination of the individual strain-optic coefficients in single-mode optical fibers,” *J. Light. Technol.*, vol. 6, no. n°1, pp. 17–20, 1988.
- [10] N. Lagakos and R. Mohr, “Stress optic coefficient and stress profile in optical fibers,” *Appl. Opt.*, vol. 20, no. 13, pp. 2309–2313, 1981.
- [11] S. Acheroy, M. Patrick, G. Thomas, H. Ottevaere, H. Thienpont, and F. Berghmans, “On a possible method to measure the radial profile of the photoelastic constant in step-index optical fiber,” in *Optical Sensing and Detection III*, 2014.
- [12] S. Acheroy, P. Merken, H. Ottevaere, T. Geernaert, H. Thienpont, and F. Berghmans, “Influence of measurement noise on the determination of the radial profile of the photoelastic coefficient in step-index optical fibers,” *Appl. Opt.*, vol. 52, no. 35, pp. 8451–9, 2013.
- [13] Chu and Whitbread, “Measurement of stresses in optical fiber and preform,” *Appl. Opt.*, vol. 21, no. 23, pp. 4241 – 4245, 1982.
- [14] K. Tatekura, “Determination of the index profile of optical fibers from transverse interferograms using Fourier theory,” *Appl. Opt.*, vol. 22, no. 3, pp. 460 – 463, 1983.
- [15] H. Poritsky, “Analysis of thermal stresses in sealed cylinders and the effect of viscous flow during anneal,” *Physics (College. Park. Md.)*, vol. 5, pp. 406 – 411, 1934.
- [16] S. Acheroy, P. Merken, T. Geernaert, H. Ottevaere, H. Thienpont, and F. Berghmans, “Algorithms for determining the radial profile of the photoelastic coefficient in glass and polymer optical fibers,” *Opt. Express*, vol. 23, no. 15, p. 18943, 2015.
- [17] S. Acheroy, P. Merken, H. Ottevaere, T. Geernaert, H. Thienpont, C. A. F. Marques, D. J. Webb, P. Gang-Ding, M. Pawel, and F. Berghmans, “Thermal effects on the photoelastic coefficient of polymer optical fibers,” *Opt. Lett.*, vol. 41, no. 11, pp. 2517–2520, 2016.
- [18] “<http://i-fiberoptics.com/fiber-detail.php?id=120>.”
- [19] “<http://www.paradigmoptics.com/>.”
- [20] W. Wu, Y. Luo, X. Cheng, X. Tian, W. Qiu, B. Zhu, G. Peng, and Q. Zhang, “Design and fabrication of single mode polymer optical fiber gratings,” vol. 12, no. 8, pp. 1652–1659, 2010.